Eighth Australasian Fluid Mechanics
Conference, University of Newcastle,
N.S.W., 28 November/2 December 1983.

SLENDER BODY THEORY IN MUCOCILIARY TRANSPORT

G.R. FULFORD AND J.R. BLAKE

DEPARTMENT OF MATHEMATICS

THE UNIVERSITY OF WOLLONGONG, WOLLONGONG, N.S.W. 2500 AUSTRALIA

SUMMARY Cilia are the major propulsive mechanism for transport of mucus in the lung. Using some recent results in slender body theory at low Reynolds number a mathematical model of the cilia sublayer is developed which incorporates a realistic cilia beat cycle. This model is used to predict mean velocity profiles in the sublayer.

1 INTRODUCTION

An important part of the body's defence against foreign particles, such as dust and bacteria, is the mucociliary clearance system in the airways of the lung. The epithelium (surface) of the respiratory tract is lined with cilia which beat like miniature oars, propelling mucus towards the opening of the trachea. Thus, foreign particles, which stick to the mucus are removed from the body. The popular conception of mucociliary transport is that of a two layered system with the cilia beating in a watery like periciliary region above which flows a layer of mucus (see fig.1.). Clearly, the fundamental problem in mucociliary transport for physiologists and fluid dynamicists alike is to gain a better understanding of the interaction of cilia and mucus and the consequent mucous flow rates.

Mucus is secreted by goblet cells which are interspersed with the more numerous ciliated cells which form the epithilium of the respiratory tract. Mucus is composed mainly of long chain glycoproteins and salts in a suspension of water. Thus it is an extremely complicated viscoelastic fluid which exhibits shear thinning properties. Extensive research has been carried out on the chemical composition and the rheological properties of mucus (see e.g., Silberberg 1982) although, until recently, far less attention has been paid to the interaction of mucus and cilia. Although we recognise that the viscoelasticity of mucus may play an important role in mucociliary transport we will model the mucous layer as a Newtonian fluid with a viscosity several orders of magnitude higher than the fluid in the periciliary layer.

Cilia are long flexible cellular projections which line the epithelia of the respiratory tract. They may also be found in other parts of the body where they have important and diverse physiological functions such as ovum transport in the oviduct and circulation of cerebrospinal fluid in the ventricles of the brain. In the animal kingdom, cilia are the primary mode of transport for certain single cell organisms (e.g., Paramecium). Although water propelling cilia have very similar internal structures to respiratory tract cilia, the latter are generally much shorter, usually within the range 5-8μm in length.

Recently, Sanderson and Sleigh (1981) have observed the cilia beat cycle in the rabbit trachea. It appears to be a three dimensional beat consisting of a fast effective stroke in which the cilium is fully extended and rotates in a vertical plane about its base. In the slower return stroke the cilium bends closer to the

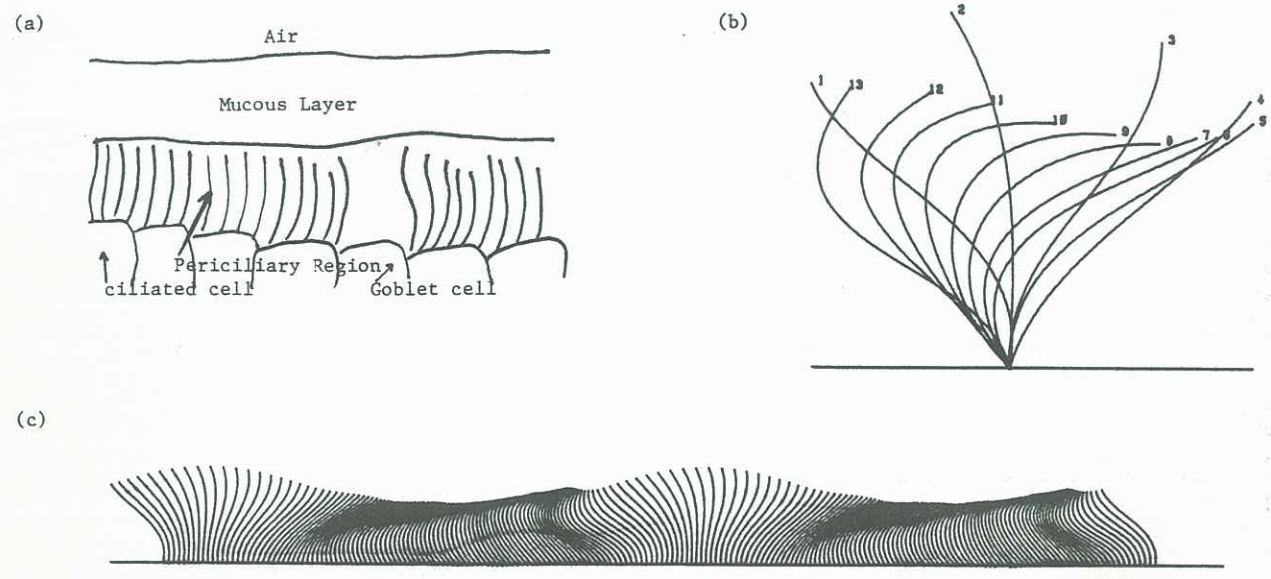

Figure 1 (a) Schematic diagram of the two-layer conception of mucociliary transport.
(b) Computer generated cilia beat cycle.
(c) Computer generated metachronal wave of ciliary activity using 100 cilia per wavelength.

epithelium and rotates back to its starting point. The cilia beat frequency ranges between approximately 10-20 Hz. In the model presented in this paper the planar beat pattern illustrated by Sleigh (1977) (see fig.1.) will be used.

We represent the ciliary beat cycle by using a method developed by Blake (1972) by assuming that the position vector $\underline{\xi}(s,t)$ for a point on the cilium (where s measures arc length from the base of the cilium and t is time) may be expanded in the Fourier series

$$\underline{\xi}(s,t) = \tfrac{1}{2}\underline{a}_o(s) + \sum_{n=1}^{N} \underline{a}_n(s)\cos n\sigma t + \underline{b}_n(s)\sin n\sigma t \qquad (1)$$

where σ is the angular beat frequency and

$$\underline{a}_n(s) = \sum_{m=1}^{M} \underline{a}_{mn} s^m \quad \text{and} \quad \underline{b}_n(s) = \sum_{m=1}^{M} \underline{b}_{mn} s^m . \qquad (2)$$

The vector constants $\underline{a}_{mn}$ and $\underline{b}_{mn}$ are determined from a Fourier-least squares procedure on the data obtained at 13 equal time intervals by Sleigh (1977). The computer generated cilia beat cycle is illustrated in fig.1.

Earlier attempts to model mucociliary transport include those of Barton and Raynor (1967) and the envelope approach of Ross (1971) but these models fail to include a realistic representation of the ciliary beat (see Blake 1975 for a discussion of the important factors in mucociliary transport). Recently there has been some controversy surrounding the question of whether the cilia actually penetrate the mucous layer. This problem was addressed by Blake and Winet (1980) using a simple mathematical model. They found that penetration significantly increases transport rates. In this paper we improve upon their model by incorporating a realistic ciliary beat pattern into the theory although in this preliminary work, only the non-penetration case is considered.

TABLE 1 Data on lung cilia

Length 5-8 μm Radius 0.1 μm
Spacing 0.3-0.4 μm Beat frequency 10-20 Hz
Wavelength of metachronal wave 20-40 μm
No. of cilia per wavelength 100
Depth of periciliary layer: 5-8 μm

2 SLENDER BODY THEORY

In this section we will present some recent results in slender body theory at low Reynolds number (Fulford and Blake 1983) and discuss their relevance to fluid dynamical models of mucociliary transport. Of particular importance is the effect of the presence of an interface between two immiscible viscous fluids on the drag on a slender body.

We are concerned with the following model problem. A slender body of length 2ℓ and circular cross section (radius R_o) has its midpoint located at a distance h from the interface in a fluid of viscosity μ_1. Above the interface is a fluid of viscosity μ_2 (see fig.2.). We will assume that the interface $x_3=0$ is perfectly flat.

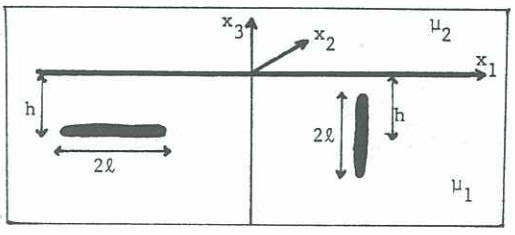

Figure 1 Slender body oriented (a) parallel and (b) perpendicular to a flat interface.

The relevant equations of motion for low Reynolds number flow are the Stokes flow equations

$$\nabla p = \mu\nabla^2\underline{u}$$
$$\nabla.\underline{u} = 0 \qquad (3)$$

where p is the pressure, μ the dynamic viscosity and $\underline{u}$ the velocity vector.

We solve these equations by placing a distribution of Stokeslets (plus appropriate image singularities) along the centre line of the slender body. It is intended merely to provide an outline of the solution technique in this paper; a far more detailed description may be found in Fulford and Blake (1983). The velocity field around the body may be written as

$$u_i(\underline{x}) = \int_{-\ell}^{\ell} F_j(s)G_{ij}(\underline{x},s)ds \qquad (4)$$

where G_{ij} is the Green's function which satisfies the boundary conditions of continuous tangential velocity and stress across the interface $x_3=0$ and zero normal velocity on the interface. By substituting the no-slip boundary condition, $\underline{u}=\underline{U}$ on the surface of the slender body into (4) we obtain a set of first kind Fredholm integral equations for the force distribution $\underline{F}(s)$. An approximate solution to these may be obtained by assuming the asymptotic expansion

$$\underline{F}(s) = \epsilon\underline{F}^{(1)} + \epsilon^2\underline{F}^{(2)} + \ldots$$

where ϵ, defined by $\epsilon = [\ell n(2\ell/R_o)]^{-1}$, is a small parameter when R_o is small compared with ℓ. Finally, the total drag on the slender body is obtained by integrating the force distributions over the length of the slender body.

The following is a summary of the results of these calculations. The drag on the slender body may be written in the form $D_T = C_T\mu_1 UL$ or $D_N = C_N\mu_1 UL$ where the subscripts T and N refer to whether the bulk movement of fluid relative to the slender body is tangent or normal to the axis of the body and $L=2\ell$ is the length of the slender body. The resistance coefficients are given by

$$C_T = \frac{2\pi\epsilon}{1+\epsilon(-\frac{1}{2}+\frac{1}{2}I)} \quad \text{or} \quad C_N = \frac{4\pi\epsilon}{1+\epsilon(\frac{1}{2}+\frac{1}{2}I)} \qquad (5)$$

where I are the interface correction terms defined as follows:

(i) for parallel orientation and motion in the x_1 direction

$$I_1'' = \left(\frac{\theta-1}{\theta+1}\right)\left[2\sinh^{-1}\frac{\ell}{h} - 3\left(1+\frac{h^2}{\ell^2}\right)^{\frac{1}{2}} + \frac{3h}{\ell}\right] + \frac{\theta}{\theta+1}\left[\frac{1}{2}\frac{h}{\ell} - \frac{h^2}{2\ell^2}\left(1+\frac{h^2}{\ell^2}\right)^{-\frac{1}{2}}\right] \qquad (6)$$

where θ is the ratio of viscosities μ_2/μ_1.

(ii) for parallel orientation and motion in the x_3 direction

$$I_3'' = 2\sinh^{-1}\frac{\ell}{h} + \frac{\theta}{\theta+1}\left(1+\frac{h^2}{\ell^2}\right)^{-\frac{1}{2}} \qquad (7)$$

(iii) for perpendicular orientation and motion in the x_1 direction

$$I_1^{\perp} = \left(\frac{\theta-1}{\theta+1}\right)\left[\left(\frac{h}{\ell}+1\right)\ell n\left(1+\frac{\ell}{h}\right) + \left(\frac{h}{\ell}-1\right)\ell n\left(1-\frac{\ell}{h}\right)\right] + \frac{1}{2}\frac{\theta}{\theta+1}\frac{\ell}{h} \qquad (8)$$

and (iv) for perpendicular orientation and motion in

the x_3 direction

$$I_3^{\perp} = \left[\left(\frac{h}{\ell}+1\right)\ell n\left(1+\frac{\ell}{n}\right)+\left(\frac{h}{\ell}-1\right)\ell n\left(1-\frac{\ell}{h}\right)\right]+\frac{1}{2}\frac{\theta}{\theta+1}\frac{\ell}{h}. \quad (9)$$

In fig.3. we have plotted the variation of the drag with respect to distance from the interface for the values $\theta = 1000$, which is relevant to mucociliary transport, and $\theta = 0$, which is relevant to the situation where there is no mucous layer. As the distance between the slender body and the interface diminishes the drag changes more rapidly for parallel orientation than for perpendicular orientation. We can imagine the effective stroke of the ciliary beat as a slender body oriented perpendicular to the interface and moving in the x_1 direction and the return stroke as a slender body oriented parallel to the interface moving in the opposite direction. From fig.3. it appears that the return stroke is approximately the right distance from the interface so that the interface effects, although increasing the drag in both cases, may cancel each other out.

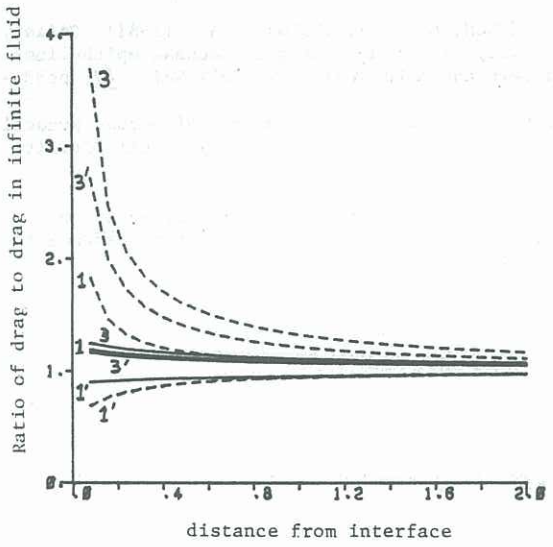

Figure 3 Drag on a slender body. The primed numbers are for $\theta = 0$ and unprimed for $\theta = 1000$.
--- Parallel orientation
—— Perpendicular orientation.

3 CILIA SUBLAYER MODEL

In our model of the periciliary region we consider a doubly infinite array of cilia (of length L) which are attached to the plane $x_3 = 0$. The cilia are aligned so that they beat in the x_1-direction and the cilia spacing in the x_1 and x_2 directions are a and b respectively. If $\underline{\xi}(s,t)$ describes a point on a single cilium with base at the origin then we can model an antiplectic metachronal wave by defining the quantity

$$\underline{\xi}'(s,t) = (ma,nb,0) + \underline{\xi}(s,\tau),\ m,n = 0,1,2,\ldots$$

where $\tau = kma + \sigma t$ (see fig.1.). The frequency of the wave is $2\pi/\sigma$ and the wavelength is $\lambda = 2\pi/k$. We will assume that the cilia are beating in a two-fluid system where the lower fluid (periciliary layer) is a Newtonian fluid with viscosity μ_1 and depth H_1 and the mucous layer is taken to be a Newtonian fluid of a much higher viscosity μ_2 and depth H_2. The interface between the two fluids and the free surface are both assumed to be flat.

The Stokes flow equations (3) are solved using a distribution of singularities (plus appropriate images) along the centre line of each cilium which are in turn summed over the doubly infinite array, giving an expression for the velocity $\underline{u}(\underline{x},t)$ as

$$u_i(\underline{x},t) = \sum_{n=-\infty}^{\infty}\sum_{m=-\infty}^{\infty}\int_0^L G_{ij}(\underline{x},\underline{\xi}')F_j(\underline{\xi}')ds \quad (10)$$

where $\underline{F}$ is the force per unit length acting on a cilium and G_{ij} is the appropriate Green's function. Given that there are N cilia per wavelength then by rearranging (10) and using Poisson's summation formula (for details of this procedure see Blake 1977) we obtain for the average velocity (in the x_1 and x_2 directions)

$$U_1(x_3,t) = \frac{1}{Nab}\sum_{n=1}^{N}\int_0^L \frac{1}{\mu_1}K\left(x_3,\xi_3^n\right)F_1\left(\xi_3^n\right)ds \quad (11)$$

where $\underline{\xi}^n$ is the n^{th} cilia in one wavelength and N is the total number of cilia in one wavelength and the "averaged Green's function" $K(x,y)$ is defined by

$$K(x,y) = \begin{cases} x & 0 < x < y < L \\ y & y < x < H_2 \end{cases}. \quad (12)$$

Note that if $x_3 > L$ then U_1 is constant.

The force distribution on each cilium F_1 is obtained using resistive force theory. In practice the force acting is determined by considering segments of the cilium and equating this to the force that would act on a segment of a straight slender body of the same length and radius of the cilium. An expression for F_1 (from Blake 1972) is

$$F_1 = C_T\left(\gamma - (\gamma-1)\frac{\partial\xi_1}{\partial s}\frac{\partial\xi_k}{\partial s}\right)V_k L\mu_1 \quad (13)$$

where C_T is the tangential resistance coefficient and γ is the ratio of normal to tangential resistance. For an approximation to the local velocity V_k we use

$$V_k = \frac{\partial\xi_k}{\partial t} - \delta_{k1}U_1 \quad (14)$$

where U_1 is the 'average' velocity in the cilia sublayer. This approximation is justified since the dominant forces are acting in the upper part of the periciliary layer where the oscillatory component of the velocity is small compared to the mean flow.

Substitution of (13) and (14) into (11) and scaling the length variables with respect to L and the velocity with respect to σL yields the integral equation for the average velocity U_1,

$$U_1(x_3,t) + \sum_{n=1}^{N}\int_0^1 T\left[\gamma-(\gamma-1)\left(\frac{\partial\xi_1^n}{\partial s}\right)^2\right]U_1\left(\xi_3^n\right)K\left(x_3,\xi_3^n\right)ds$$

$$= \sum_{n=1}^{N}\int_0^1 T\left\{\left[\gamma-(\gamma-1)\left(\frac{\partial\xi_1^n}{\partial s}\right)^2\right]\frac{\partial\xi_1^n}{\partial t} - (\gamma-1)\frac{\partial\xi_1^n}{\partial s}\frac{\partial\xi_3^n}{\partial s}\frac{\partial\xi_3^n}{\partial t}\right\}K\left(x_3,\xi_3^n\right)ds$$

where the density parameter $T = C_T/(Nab)$. Note that the explicit dependence on the viscosity of the lower region μ_1 has cancelled out although C_T and γ may depend on the ratio of viscosities θ. We solve this equation by discretising both x_3 and s into equal intervals. The integral is calculated using the trapezoidal rule and linear interpolation is used to obtain $U_1(\xi_3)$ in terms of $U_1(x_3)$.

4 RESULTS

Using the data in Table 1 we calculate $\epsilon \doteq 0.25$. If, as a first approximation, we use only first order results in (5) we obtain $T \doteq 7$ and $\gamma = 2$. The predictions of the model using this value is illustrated in fig.4. Note how the major contribution to the flow occurs in the region where the effective stroke protrudes above the return stroke (i.e., $x_3 = .7$ to 1). We obtain a non-dimensional velocity of about 1 for the mucous layer which corresponds to a velocity of about 300 μm/sec.

which although a little high, appears to agree with observed values (Sleigh 1977).

One might anticipate a better approximation would be to use the full expressions in (5) without the interface correction terms. This yields $T = 8.28$ and $\gamma = 1.4$, however this change of parameter values does not greatly influence the velocity profile. To include the effect of the interface on the resistance coefficients we can adopt the following strategy. For the effective stroke we assume that the correction term is that for a slender body oriented perpendicular to the interface moving in the x_1 direction where as for the return stroke we use the correction terms for a slender body parallel to the interface and moving in the x_1 direction. For $\theta = 1000$ we used $T = 12.0$ and $\gamma = 1.3$ for the effective stroke and $T = 9.8$ and $\gamma = 2.0$ for the return stroke. Similarly, for $\theta = 0$ we used $T = 10.5$ and $\gamma = 1.0$ for the effective stroke and $T = 7.2$ and $\gamma = 2.5$. Neither case showed any appreciable variation from the $T = 7$, $\gamma = 2$ velocity profile.

Several extensions of this model suggest themselves for further research. Foremost among these would include the incorporation of a three dimensional beat cycle and also an adaption of the model to account for penetration of the cilia into the mucous layer. In order to complete the latter, however further theory concerning the penetration of a slender body through an interface needs to be developed.

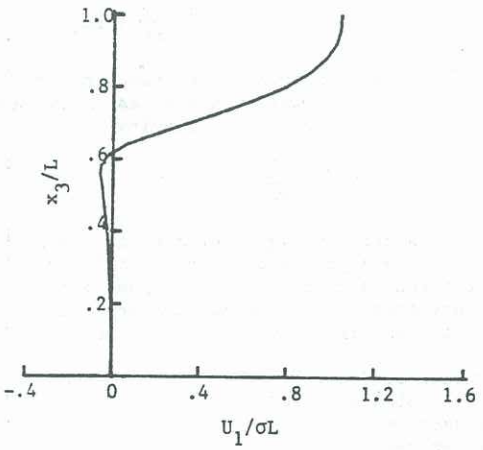

Figure 4 Mean velocity profile in periciliary region with $T = 7$ and $\gamma = 2$.

5 REFERENCES

BARTON, C. and RAYNOR, S. (1967) Analytical investigation of cilia induced mucous flow. Bull. Math. Physics, 29, pp419-427.

BLAKE, J.R. (1972) A model for the micro-structure in ciliated organisms. J. Fluid Mech., 55, pp1-23.

BLAKE, J.R. (1975) On the movement of mucus in the lung. J. Biomech., 8, pp179-190.

BLAKE, J.R. and WINET, H. (1980) On the mechanics of micro-ciliary transport. Biorheol., 17, pp125-134.

FULFORD, G.R. and BLAKE, J.R. (1983) On the motion of a slender body near an interface between two immiscible liquids at very low Reynolds numbers. J. Fluid Mech., 127, pp203-217.

ROSS, S.M. (1971) A wavy wall analytical model of muco-ciliary pumping. PhD Thesis, John Hopkins University.

SANDERSON, M.J. and SLEIGH, M.A. (1981) Ciliary activity of cultured rabbit tracheal epithelium: beat pattern and metachrony. J. Cell Sci., 47, pp331-347.

SILBERBERG, A. (1982) Rheology of mucus, mucociliary interaction and ciliary activity. Cell Motility Supp., 1, pp25-28.

SLEIGH, M.A. (1977) The nature and action of respiratory tract cilia. Respiratory Defence Mechanisms. Marcel Dekker Inc., N.Y.